CHEMISTRY
A EUROPEAN JOURNAL

DOI: 10.1002/chem.200801833

The Interplay between Steric and Electronic Effects in S_N2 Reactions

Israel Fernández,*[b, c] Gernot Frenking,*[b] and Einar Uggerud*[a]

Abstract: Quantum chemical calculations for S_N2 reactions of H_3EX/X^- systems, in which E = C or Si and X = F or Cl, are reported. In the case of the carbon system we also report on bulkier species in which the hydrogen atoms are substituted by methyl groups. It is shown how the variation in the individual energy terms of the Morokuma/Ziegler energy decomposition analysis (EDA) scheme along the reaction coordinate from reactants to products provides valuable insight into the essential changes that occur in the bond-breaking/bond-forming process during S_N2 reactions. The EDA results for the prototypical S_N2 reaction of the systems $[X\cdots R_3E\cdots X]^-$, in which the interacting fragments are $[X\cdots X]^{2-}$ and $[R_3E]^+$, have given rise to a new interpretation of the factors governing the reaction course. The EDA results for the carbon system (E = C) show that there is less steric repulsion and stronger electrostatic attraction in the transition structure than in the precursor complex and that the energy increase comes mainly from weaker orbital interactions. The larger barriers for systems in which R_3 is bulkier also do not arise from increased steric repulsion, which is actually released in the transition structure. It is rather the weakening of the electrostatic attraction, and in particular the loss of attractive orbital interactions, that are responsible for the activation barrier. The D_{3h} energy minima of the silicon homologues $[XH_3SiX]^-$ is driven by the large increase in the electrostatic attractions and also of stronger orbital interactions, while the steric interactions is destabilizing.

Keywords: energy decomposition analysis · molecular modeling · nucleophilic substitution · reaction mechanisms · steric hindrance

Introduction

The prototype S_N2 reaction is well known to all chemists, and constitutes a fundamental point in common understanding of chemical reactivity. In this respect, the work of Ingold, Hughes and co-workers was essential, in the introduction of the terms S_N1, S_N2, E1 and E2.[1] These terms still form the cornerstones of the conceptual framework in which a wide range of organic and biological reactions are understood, and they also define a central part of the traditional curriculum in organic chemistry worldwide.[2–4]

Although the original definitions of S_N1, S_N2, E1 and E2 are accurate enough, the factors influencing the rates and mechanistic details of these reaction types are still incompletely understood. The same is true for the understanding of the factors that place a particular reaction in the landscape between these extreme mechanistic alternatives, and thereby determine product distributions and stereoselectivities. To some degree this is the result of incomplete knowledge, but the vagueness of the language that is used to describe the phenomena under study also hampers progress. Organic chemistry has a tradition of applying operationally defined terminology. Typical examples include "aromaticity" and "steric", "inductive" and "resonance" effects, which have been termed "unicorns" in chemistry because everybody seems to know what they mean although they are not observables.[5] These definitions lack the rigorous mathematical accuracy more typical of physical chemistry and physics. This cultural difference becomes apparent when quantum mechanics is applied to organic reactions, because none of the above terms corresponds to a physical observable. Sometimes this ambiguity gives rise to interesting and fruitful discussions of great scientific value, but more often it

[a] Prof. E. Uggerud
Massespektrometrilaboratoriet og
Senter for teoretisk og beregningsbasert kjemi (CTCC)
Kjemisk institutt
Universitetet i Oslo, Postboks 1033 Blindern, 0315 Oslo (Norway)
Fax: (+47) 22 8554 41
E-mail: einar.uggerud@kjemi.uio.no

[b] Dr. I. Fernández, Prof. Dr. G. Frenking
Fachbereich Chemie, Philipps-Universität Marburg
Hans-Meerwein-Strasse, 35043 Marburg (Germany)

[c] Dr. I. Fernández
Present address:
Departamento de Química Orgánica
Facultad de Química, Universidad Complutense
28040 Madrid (Spain)

creates the potential for alternative interpretations with unforeseen misunderstandings in its wake.

Fortunately, insight into the physical factors steering S_N2 reactivity has become much better during the last decades. Through the study of small model systems in the gas phase, isolated from influential solvent effects[6]—either experimentally by mass spectrometry[7–13] or theoretically by quantum chemical calculations[14–18]—it has become possible to probe the relationship between the structural features of the reacting molecules and their reactivity in greater detail and at a more fundamental level than before. As an example, the periodic variation in reactivity is in many cases different between solution and gas phase, and gas-phase reactivity trends have been explained in terms of the essential molecular properties of nucleophiles and substrates.[19–22] It has proven extremely useful to deconvolute the intrinsic kinetic barrier from the thermodynamic driving force by comparing non-identity and identity S_N2 reactions.[15] The observed trends are understood at this more fundamental level, but their translation into the well established terminology of organic chemistry represents a more challenging task.

In this respect the introduction of an energy decomposition analysis (EDA) may be useful. The EDA method provides a particularly consistent approach by dividing the energy of interaction between a set of predefined fragment molecules into mathematically unambiguously defined terms that give the electrostatic, Pauli and orbital contributions.[23,24] The advantage of the EDA is that it delineates the instantaneous interaction energy between the fragments, which makes it possible to compare the energy values directly without using an external standard. In this way it has been possible to compare the strengths of conjugation, hyperconjugation and aromaticity in π-conjugated systems[25,26] and to analyse the nature of a chemical bond in terms of electrostatic attraction and orbital (covalent) bonding, which can be further divided into σ-, π- and possibly δ-bonding.[27–31] Bickelhaupt and co-workers pioneered the systematic use of this approach for gas-phase E2 and S_N2 reactions.[25] By applying EDA in combination with their own activation strain analysis for S_N2 reactions, for example, they were able to provide insight into how the passage through a critical transition structure (TS) affects the different categories of interactions between a chosen molecular subgroup of atoms. From this analysis they suggested how steric and electronic effects may contribute to the barrier height.[32,33]

In the preparation for an energy decomposition analysis of a chemical reaction, three issues must be given careful consideration. Firstly, the single determinant wavefunction to be used must be shown to be sufficiently accurate for the purpose. Secondly, one needs to be extremely careful not to over-interpret the outcome of the analysis when translating it into common organic chemistry terminology, as discussed above. Thirdly, the particular choice of molecular fragments for the EDA needs attention, because the absolute values of each of the energy terms will depend intimately on this. Here we consider that the correspondence between the energies and properties of the TS as well as the reactant and product states of the S_N2 reaction $Y^- + RX \rightarrow X^- + RY$ can best be characterised from the fully separated fragments $X^- + R^+ + Y^-$.[21] Our choice of fragments differs from that used by Bickelhaupt and co-workers, who decomposed the energy of interaction of X^- and RY. In addition to comparing all energies to common origin, our approach has the advantage of eliminating the use of activation strain analysis as introduced by Bickelhaupt.[32] Moreover, we think that it is more realistic to consider the nascent and the breaking bonds simultaneously because they are closely associated with each other. This holds in particular for the transition structure in which the two bonds are equally important. The advantage of our approach is that it considers not only the interactions between the attacking nucleophile and the substrate, but also the energy changes in the system that arise from the breaking of the bond of the leaving group. Here we show that through capture of both effects—that is, the formation of the new bond and the concomitant rupture of the bond of the leaving group–-the information relating to the energy terms responsible for the activation barrier becomes significantly different from that of any traditional viewpoint.

Here we analyse how the critical energy of a given S_N2 reaction depends on a number of crucial structural factors during the reaction, including the roles of the nucleophile/nucleofuge (leaving group), the substrate R, and the properties of the central atom at the reaction centre.

Experimental Section

The geometries of the molecules have been optimized at the DFT level of theory by use of the OPBE functional,[34] which has recently been recommended for modelling of S_N2 reactions involving pentacoordinate carbon in their transition structures.[35] Uncontracted Slater-type orbitals (STOs) were employed as basis functions for the SCF calculations.[36] The basis sets are of triple-ζ quality augmented by two sets of polarization functions: p and d functions for the hydrogen atoms and d and f functions for the other atoms. This level of theory is denoted as OPBE/TZ2P+. An auxiliary set of s, p, d, f and g STOs was used to fit the molecular densities and to represent the Coulomb and exchange potentials accurately in each SCF cycle.[37] The vibrational frequencies of the optimized structures have been calculated in order to investigate the natures of the stationary points. The Hessian matrices of the optimized geometries have only positive eigenvalues for a minimum on the potential energy surface, whereas a transition structure gives rise to one negative eigenvalue. The calculations were carried out with the program package ADF 2007.01.[38] For calibration purposes we also performed single-point energy calculations at the CCSD(T) level of theory by use of the triple-zeta quality def2-TZVPP basis set[39] on the OPBE/TZ2P+ geometries. These calculations were performed with the GAUSSIAN 03 suite of programs.[40]

The interactions were analysed by means of the energy decomposition analysis (EDA) of ADF, which was developed by Ziegler and Rauk[24] by a procedure similar to that suggested by Morokuma.[23] EDA has proven to give important information about the nature of the bonding in main-group compounds and transition-metal complexes.[25–31] The focus of the bonding analysis is the instantaneous interaction energy (ΔE_{int}) of the bond, which is the energy difference between the molecule and the fragments in the electronic reference state and frozen geometry of the compound. The interaction energy can be divided into three main components:

$$\Delta E_{int} = \Delta E_{elstat} + \Delta E_{Pauli} + \Delta E_{orb} \quad (I)$$

ΔE_{elstat} gives the electrostatic interaction energy between the fragments, calculated by use of the frozen electron density distribution of the fragments in the geometry of the molecules. The second term in Equation (I), ΔE_{Pauli}, refers to the repulsive interactions between the fragments, which are caused by the fact that two electrons with the same spin cannot occupy the same region in space. ΔE_{Pauli} is calculated by enforcing the Kohn–Sham determinant on the superimposed fragments so that they obey the Pauli principle by antisymmetrization and renormalization. The stabilizing orbital interaction term (ΔE_{orb}) is calculated in the final step of the energy partitioning analysis when the Kohn–Sham orbitals relax to their optimal form. This term can be further partitioned into contributions from the orbitals belonging to different irreducible representations of the point group of the interacting system. The interaction energy (ΔE_{int}) can be used to calculate the bond dissociation energy (D_e) by adding ΔE_{prep}, which is the energy necessary to promote the fragments from their equilibrium geometry to the geometry in the compounds [Eq. (II)]. The advantage of using ΔE_{int} instead of D_e is that the instantaneous electronic interaction of the fragments is analysed, which yields a direct estimate of the energy components.

$$-D_e = \Delta E_{prep} + \Delta E_{int} \quad (II)$$

Results

Effect of nucleophile: A typical gas-phase S_N2 reaction is characterised by the so-called double-well potential energy function[41] as illustrated in Figure 1. On the way from infinitely separated reactants X^-+RX to the TS there is a potential energy minimum corresponding to the ion/molecule complex $[XR\cdots X]^-$, which has one long distance R···X between the central atom of the group R and the nucleophile X and one short interatomic distance X–R between the leaving group X and R. The latter distance is usually only slightly longer than in the equilibrium structure. The degenerate substitution reaction from $[XR\cdots X]^-$ to $[X\cdots RX]^-$ passes through the transition structure $[X\cdots R\cdots X]^-$ in which the R···X distances have the same value. The energy difference between the transition structure and the separated reactants X^-+RX gives the critical energy ($E^{\#}$). In the absence of a central energy barrier this function collapses into a single-well function.

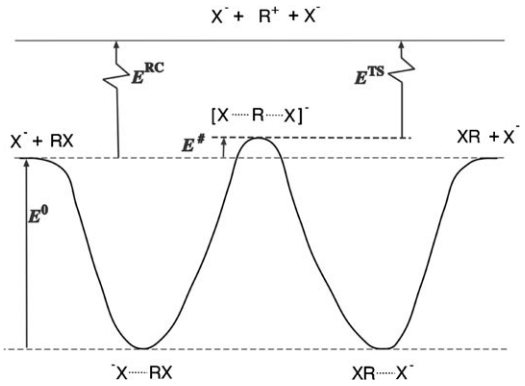

Figure 1. Depiction of the symmetric double-well potential diagram of an identity S_N2 reaction.

Table 1 shows the value of the critical energies ($E^{\#}$) for the various reactions investigated in this study. We will start by discussing the results for the reactions:

$$F^- + CH_3F \rightarrow FCH_3 + F^- \quad (1)$$

$$Cl^- + CH_3Cl \rightarrow ClCH_3 + Cl^- \quad (2)$$

Previous investigations have shown that Reaction (2) has a lot in common with Reaction (1).[6] The barrier of Reaction (2) is ≈ 5 kcal mol^{-1} higher than for Reaction (1), and the $E^{\#}$ value for the chlorine system is 0.1 kcal mol^{-1} at CCSD(T)/TZVPP. Like Swart et al., we find that the hybrid density functional OPBE/TZ2P+ offers a computationally attractive alternative in combining sufficient accuracy with economy.[35,42] The critical energy compares favourably with those obtained for the highly correlated wave function CCSD(T)/TZVPP//OPBE/TZ2P+ (Table 1). Moreover, and importantly for our purposes, OPBE gives rise to a one-determinant formulation of the wave function consistent with the EDA approach outlined above.

Table 1. Critical energies ($E^{\#}$; see Figure 1) in kcal mol^{-1}.

System	OPBE/TZ2P+	CCSD(T)/def2-TZVPP//OPBE/TZ2P+
$[F\cdots Me\cdots F]^-$	−4.5	−5.4
$[Cl\cdots Me\cdots Cl]^-$	+2.4	+0.1
$[F\cdots Et\cdots F]^-$	−0.5	−4.0
$[F\cdots i\text{Pr}\cdots F]^-$	+3.0	−2.6
$[F\cdots t\text{Bu}\cdots F]^-$	+10.0	+2.5
$[F\cdots SiH_3\cdots F]^-$	−58.3	−66.5
$[Cl\cdots SiH_3\cdots Cl]^-$	−27.0	−31.3

Our EDA investigation is anchored to the CH_3^++$[X\cdots X]^{2-}$ fragments. This choice has the advantage that both the reactant and the TS can be analysed from a common reference point and because the key physical quantity, the critical energy, is the difference in the relevant energy terms; $E^{\#} = E^{RC} - E^{TS}$, as is evident from Figure 1. In addition, this allows for a straightforward analysis of the binding situation at any point along the entire reaction pathway. There are three particular points along the calculated pathway $[CH_3\cdots X]^-$.

1) At $r(C\cdots X) = \infty$ the EDA values are associated with the formation of CH_3X from the components R^+ and X^-.
2) The second key point along the minimum reaction path is the transition structure for the nucleophilic substitution where both C–X distances have the same value.
3) The third point, the ion/molecule complex $[XCH_3\cdots X]^-$, lies in-between points 1) and 2). It corresponds to a true minimum energy point for X = F, Cl.

Despite the fact that the ion/molecule complexes are minima along the reaction pathway, the details regarding their exact relationship to the topography of the potential energy surface are rather unimportant in our analysis be-

cause the following discussion focuses on the end points 1) and 2), because only these structures determine the critical energy (=the energy difference).

Figure 2a and b show the trend of the different energy terms along the pathway from the reactants starting at r(C–X)=6.0 Å to the transition structure for the degenerate S_N2 reactions CH_3X+X^- (X=F, Cl), which exhibit remarkable features. Table 2 gives the differences in the energy terms of the EDA between the approaching reactants at an early stage (r=6.0 Å) and the transition structure for the S_N2 Reactions (1) and (2) at various distances.

Perhaps the most surprising result is that the Pauli repulsion (ΔE_{Pauli}) at the transition structures is significantly *weaker* than in the beginning of the reaction. Figure 2a and b show that ΔE_{Pauli} continuously decreases along the reaction pathway. This means that the increase in the Pauli repulsion between the attacking nucleophile X^- and the H_3C^+ group in $[X\cdots H_3C\cdots X]^-$ is compensated by the weaker repulsion between the leaving group and H_3C^+. This is a very important finding, because the steric repulsion has previously been identified as a crucial factor for the S_N2 reaction.[32,33]

Another intriguing finding is the similarity between the curves for the total interaction energy (ΔE_{int}) and the electrostatic term (ΔE_{elstat}), which holds particularly for X=F (Figure 2a). The absolute values and the trend of ΔE_{int} and ΔE_{elstat} in this system closely resemble each other. This is surprising because nucleophilic substitution is usually discussed in terms of orbital interactions in which the σ HOMO of the nucleophile interacts with the σ* LUMO of the substrate. Figure 2a shows that the orbital interactions in the system $[XH_3C\cdots X]^-$ along the reaction pathway are quite large and that, as would be expected, they come mainly from the $a_1(\sigma)$ orbitals, whereas the e(π) bonding, which originates from the donation of the fluorine p(π) orbitals into the π* orbital of CH_3^+ is much weaker. However, the change in the attractive orbital interactions appears to be compensated by the Pauli repulsion, which originates from the interactions between the occupied orbitals of the fragments. Figure 2 shows that the curves for ΔE_{Pauli} look like mirror images of the ΔE_{orb} curves.

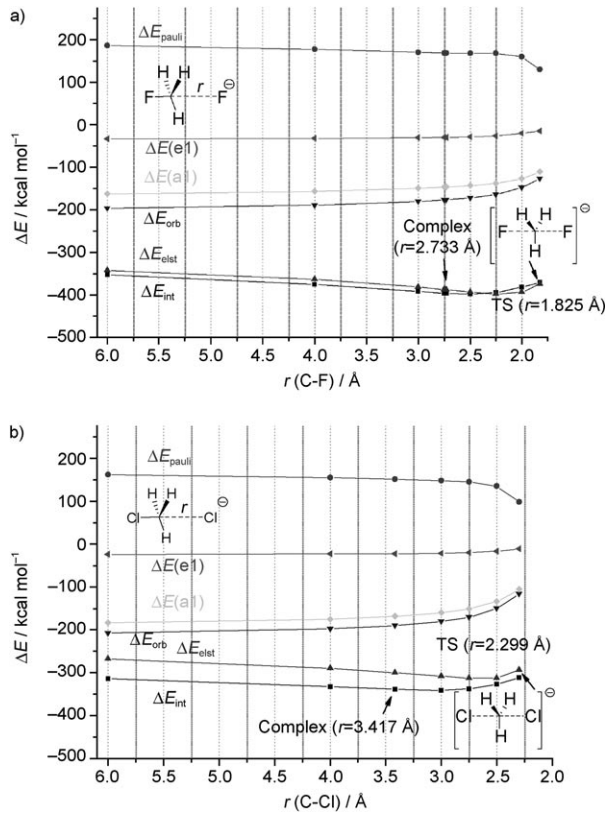

Figure 2. EDA plots for the CH_3X+X^- S_N2 reactions computed at the OPBE/TZ2P+ level. a) X=F, b) X=Cl.

A closer look at Figure 2a and 2b reveals interesting details. In the region between r(C–X)=6.0 Å and the equilibrium value for the ion/molecule complex $[XH_3C\cdots X]^-$, where X=F, Cl, the interaction energy (ΔE_{int}) becomes more attractive and so does the electrostatic term (ΔE_{elstat}), while the attractive orbital interactions (ΔE_{orb}) decrease. The shape of the curves suggests that the driving force for the formation of the $[XH_3C\cdots X]^-$ complex comes from the electrostatic term (ΔE_{elstat}). The calculated numbers given in Table 2 support this. The energy values for the different terms of the system $[F\cdots H_3C\cdots F]^-$ indicate that there is a *decrease* in the attractive orbital term (ΔE_{orb}) by 19.8 kcal mol^{-1} and a decrease in the repulsive term (ΔE_{Pauli}) by 17.6 kcal mol^{-1} between r(C–X)=6.0 Å and the equilibrium value for the ion/molecule complex. This gives a net destabilization of 2.2 kcal mol^{-1}. The crucial factor that stabilizes the ion/dipole complex comes from the electrostatic attraction ($\Delta\Delta E_{elstat}$), which *increases* by 24.6 kcal mol^{-1}. A similar situation is found for the chlorine system $[Cl\cdots H_3C\cdots Cl]^-$ (Table 2). The attractive orbital interactions decrease by $\Delta\Delta E_{orb}$=17.5 kcal mol^{-1} and the Pauli repulsion decreases by $\Delta\Delta E_{Pauli}$=10.4 kcal mol^{-1}, but the electrostatic attraction increases by 32.1 kcal mol^{-1}.

In the region between the ion/molecule complex and the transition structure, the interaction energy (ΔE_{int}) becomes less attractive in the final part of the reaction coordinate (Figure 2 and Table 2). Both attractive terms ΔE_{elstat} and ΔE_{orb} decrease when the transition structure is approached, but the repulsive Pauli interactions (ΔE_{Pauli}) also decrease. The values in Table 2 show that, for the system $[F\cdots H_3C\cdots F]^-$, part of the weakening in the attractive interaction energy ($\Delta\Delta E_{int}$=25.6 kcal mol^{-1}) between the ion/molecule complex and the transition structure comes from the loss of electrostatic attraction ($\Delta\Delta E_{elstat}$=13.9 kcal mol^{-1}), whereas a larger part comes from the significant loss in attractive orbital interactions ($\Delta\Delta E_{orb}$=49.7 kcal mol^{-1}), which is not fully compensated by the decrease in the Pauli repulsion ($\Delta\Delta E_{Pauli}$=37.9 kcal mol^{-1}). This effect is more dominant in the chlorine system $[Cl\cdots H_3C\cdots Cl]^-$. Table 2 shows that, in that system, the weakening in the attractive interaction energy ($\Delta\Delta E_{int}$=27.6 kcal mol^{-1}) between the ion/molecule complex and the transition structure originates mainly from the difference between the loss of orbital attraction ($\Delta\Delta E_{orb}$=74.2 kcal mol^{-1}) and Pauli repulsion

Table 2. Change in the energy terms of the EDA for the systems $[XR_3E\cdots X]^-$ between $r(E\cdots X)=4.0$ Å and the pentacoordinated systems $[X\cdots R_3E\cdots X]^-$ in which both E–X distances are the same. Energy values in kcal mol^{-1}, distances in Å.

					CH_3F/F^-				
r(E···X)	6.0	4.0	3.0	2.75	2.73 (min)	2.5	2.25	2.0	1.825 (TS)
$\Delta\Delta E_{int}$	0.0	−22.6	−39.4	−43.3	−43.5	−45.3	−41.8	−28.7	−17.9
$\Delta\Delta E_{Pauli}$	0.0	−8.6	−16.0	−17.5	−17.6	−18.3	−18.2	−26.0	−55.5
$\Delta\Delta E_{elstat}$	0.0	−21.1	−39.5	−45.3	−45.8	−51.3	−55.8	−51.6	−31.9
$\Delta\Delta E_{Orb}$	0.0	7.1	16.2	19.6	19.8	24.3	32.2	48.9	69.5
$\Delta\Delta E_{Orb}$ (a_1)	0.0	5.8	13.6	16.3	16.5	19.8	25.2	36.1	51.3
$\Delta\Delta E_{Orb}$ (e)	0.0	1.3	2.6	3.3	3.4	4.5	7.0	12.8	18.1
$\Delta\Delta E_{prep}$	0.0	17.4	30.3	33.7	33.8	35.8	34.2	25.6	17.0
$\Delta\Delta E$	0.0	−5.2	−9.1	−9.6	−9.7	−9.5	−7.6	−3.1	−0.9
					CH_3Cl/Cl^-				
r(E···X)	6.0	4.0	3.417 (min)	3.0	2.75	2.5	2.299 (TS)		
$\Delta\Delta E_{int}$	0.0	−18.8	−25.0	−27.2	−24.1	−12.8	2.6		
$\Delta\Delta E_{Pauli}$	0.0	−6.7	−10.4	−13.8	−16.7	−26.3	−63.6		
$\Delta\Delta E_{elstat}$	0.0	−22.1	−32.1	−40.3	−44.8	−44.6	−25.5		
$\Delta\Delta E_{Orb}$	0.0	10.1	17.5	26.9	37.3	58.2	91.7		
$\Delta\Delta E_{Orb}$ (a_1)	0.0	9.2	16.0	24.4	33.3	50.7	78.7		
$\Delta\Delta E_{Orb}$ (e)	0.0	0.9	1.6	2.5	4.0	7.5	13.0		
$\Delta\Delta E_{prep}$	0.0	14.9	20.5	23.7	22.6	15.8	3.1		
$\Delta\Delta E$	0.0	−3.9	−4.5	−3.5	−1.5	3.0	5.7		
					EtF/F^-				
r(E···X)	6.0	4.0	3.0	2.75	2.5	2.25	2.0	1.870 (TS)	
$\Delta\Delta E_{int}$	0.0	−22.0	−37.6	−41.4	−42.9	−38.5	−24.2	−13.6	
$\Delta\Delta E_{Pauli}$	0.0	−10.0	−17.4	−18.9	−19.8	−22.1	−42.4	−84.5	
$\Delta\Delta E_{elstat}$	0.0	−20.1	−29.1	−33.5	−37.9	−40.1	−28.9	−3.4	
$\Delta\Delta E_{Orb}$	0.0	8.0	8.9	10.9	14.8	23.6	47.2	74.3	
$\Delta\Delta E_{Orb}$ (a′)	0.0	8.6	8.8	10.9	14.7	22.6	43.2	67.9	
$\Delta\Delta E_{Orb}$ (a″)	0.0	−0.5	0.1	0.0	0.1	1.0	4.0	6.3	
$\Delta\Delta E_{prep}$	0.0	16.6	29.5	33.0	35.1	33.2	24.1	15.2	
$\Delta\Delta E$	0.0	−5.4	−8.1	−8.4	−7.8	−5.3	−0.1	1.6	
					iPrF/F^-				
r(E···X)	6.0	4.0	3.0	2.75	2.25	2.0	1.908 (TS)		
$\Delta\Delta E_{int}$	0.0	−27.8	−40.7	−41.6	−32.5	−13.8	−6.2		
$\Delta\Delta E_{Pauli}$	0.0	−7.8	3.1	−0.4	−3.6	−47.8	−90.2		
$\Delta\Delta E_{elstat}$	0.0	−26.4	−50.7	−48.1	−47.0	−19.2	6.8		
$\Delta\Delta E_{Orb}$	0.0	6.4	6.9	6.8	18.0	53.2	77.1		
$\Delta\Delta E_{Orb}$ (a′)	0.0	8.9	13.9	12.8	22.7	54.3	76.1		
$\Delta\Delta E_{Orb}$ (a″)	0.0	−2.5	−6.9	−6.6	−4.6	−1.1	1.0		
$\Delta\Delta E_{prep}$	0.0	17.7	27.9	31.0	32.1	21.6	15.9		
$\Delta\Delta E$	0.0	−10.1	−12.8	−10.6	−0.4	7.8	9.1		
					tBuF/F^-				
r(E···X)	6.0	4.0	3.0	2.75	2.5	2.25	2.0	1.983 (TS)	
$\Delta\Delta E_{int}$	0.0	−28.8	−41.2	−34.4	−22.9	−9.8	4.2	8.6	
$\Delta\Delta E_{Pauli}$	0.0	−7.7	6.0	16.2	20.6	4.3	−60.0	−92.3	
$\Delta\Delta E_{elstat}$	0.0	−25.2	−52.5	−58.3	−57.6	−44.2	−4.3	15.4	
$\Delta\Delta E_{Orb}$	0.0	4.0	5.3	7.7	14.2	30.2	68.4	85.6	
$\Delta\Delta E_{Orb}$ (a′)	0.0	6.5	11.2	15.5	21.7	35.5	69.2	84.5	
$\Delta\Delta E_{Orb}$ (a″)	0.0	−2.5	−6.7	−7.8	−7.5	−5.3	−0.8	0.9	
$\Delta\Delta E_{prep}$	0.0	17.9	27.6	25.2	21.6	18.5	12.3	8.0	
$\Delta\Delta E$	0.0	−10.9	−13.6	−9.2	−1.3	8.7	16.5	16.6	
					SiH_3F/F^-				
r(E···X)	6.0	4.0	3.0	2.75	2.5	2.25	2.0	1.750 (min)	
$\Delta\Delta E_{int}$	0.0	−18.8	−35.8	−42.5	−51.2	−62.4	−75.5	−86.5	
$\Delta\Delta E_{Pauli}$	0.0	−4.4	−5.2	−3.0	2.5	14.2	39.4	94.4	
$\Delta\Delta E_{elstat}$	0.0	−18.6	−34.4	−40.8	−49.9	−63.9	−87.2	−128.0	
$\Delta\Delta E_{Orb}$	0.0	4.2	3.8	1.2	−3.8	−12.6	−27.7	−52.9	
$\Delta\Delta E_{Orb}$ (a_1)	0.0	2.6	1.0	−1.6	−6.3	−13.7	−24.8	−40.2	
$\Delta\Delta E_{Orb}$ (e)	0.0	1.5	2.8	2.9	2.5	1.0	−3.1	−12.7	
$\Delta\Delta E_{prep}$	0.0	12.9	19.9	21.5	23.3	26.0	29.1	34.3	
$\Delta\Delta E$	0.0	−5.9	−15.9	−21.0	−27.9	−36.7	−46.4	−52.2	
					SiH_3Cl/Cl^-				
r(E···X)	6.0	4.0	3.0	2.75	2.5	2.316 (min)			
$\Delta\Delta E_{int}$	0.0	−14.6	−25.8	−30.1	−34.8	−37.6			

Table 2. (Continued)

	SiH_3Cl/Cl^-					
$\Delta\Delta E_{Pauli}$	0.0	−6.5	−6.4	−1.0	11.8	30.4
$\Delta\Delta E_{elstat}$	0.0	−17.4	−32.8	−40.1	−51.0	−63.1
$\Delta\Delta E_{Orb}$	0.0	9.4	13.4	11.0	4.3	−5.0
$\Delta\Delta E_{Orb}$ (a_1)	0.0	6.0	5.6	3.1	−2.8	−9.4
$\Delta\Delta E_{Orb}$ (e)	0.0	3.4	7.3	7.9	7.1	−5.8
$\Delta\Delta E_{prep}$	0.0	9.2	11.3	11.7	12.5	14.0
$\Delta\Delta E$	0.0	−5.4	−14.5	−18.4	−22.3	−23.6

[a] Energy difference between r(E–X) = 6.0 Å and the equilibrium distance of the complex. [b] Energy difference between the equilibrium distance of the complex and the transition structure. [c] Energy difference between r(E–X) = 6.0 Å and the transition structure.

($\Delta\Delta E_{Pauli} = 53.2$ kcal mol^{-1}), yielding a net destabilization of 21.0 kcal mol^{-1}. The remaining contribution to the total energy increase comes from the loss of electrostatic attraction, which amounts to $\Delta\Delta E_{elstat} = 6.6$ kcal mol^{-1}. Figure 2a and b show, however, that the electrostatic attraction first significantly increases in both systems when the distance between the nucleophile and the substrate becomes shorter than in the equilibrium complex $[XH_3C\cdots X]^-$ (X = F, Cl).

The values for the overall change in the energy terms on moving from r(E–X) = 6.0 Å to the transition structure, yielding the critical energy ($E^{\#}$), indicate that the Pauli repulsion (ΔE_{Pauli}) and the electrostatic interaction (ΔE_{elstat}) actually stabilize the transition structure because the Pauli repulsion becomes weaker and the electrostatic attraction becomes stronger in the transition structure. The energy increase comes solely from the significantly weaker orbital term (ΔE_{orb}).

Effect of substrate: Below we discuss the energy changes $[F\cdots R_3C\cdots F]^-$ when R becomes bulkier than hydrogen. To this end we analysed the interaction energies for Reaction (1) (above), together with the following reactions:

$$F^- + CH_3F \rightarrow FCH_3 + F^- \quad (3)$$

$$F^- + CH_3CH_2F \rightarrow FCH_2CH_3 + F^- \quad (4)$$

$$F^- + (CH_3)_2CHF \rightarrow FCH(CH_3)_2 + F^- \quad (5)$$

$$F^- + (CH_3)_3CF \rightarrow FC(CH_3)_3 + F^- \quad (6)$$

Table 1 shows that the barrier increases with the size of the alkyl group, thus following the normal reactivity trend (Table 1). There are some quantitative differences between the absolute values of the critical energies between OPBE and CCSD(T) but the relative trends are the same. We therefore gauge that OPBE provides sufficiently consistent results to allow for a reliable EDA trend analysis. To what degree is this trend the result of the steric bulk of the substituents, and to what extent is it due to electronic effects from the methyl substituents at the carbon?

The energy profile for Reaction (1) has already been given in Figure 2a. Figure 3 a–c show the changes in the EDA components for Reactions (4)–(6). The minima observed for ΔE_{int} do not coincide exactly with the minimum-energy geometries for $[F\cdots R_3CF]^-$ for two reasons. Firstly, the effect of ΔE_{prep} is not considered (we will return to this). Secondly, the data presented here are the result of enforcing a linear X–C–X arrangement. The optimum complex geometries deviate somewhat from this, although not to a very significant degree, and the complexes do essentially have the correct $[F\cdots R_3CF]^-$ arrangements. For the purpose of the bonding analysis in this work we think that the enforcement of a linear X–C–X arrangement has a negligible effect on the conclusions drawn.

Both Table 2 and Figure 3 show that the decrease in the attractive interaction energy ($\Delta\Delta E_{int}$) between the reactants and the transition structures has the expected order $CH_3 < CH_3CH_2 < (CH_3)_2CH < (CH_3)_3C$. The increase in the activation barrier thus directly correlates with the intrinsic interaction energies. Figure 2a and Figure 3 a–c suggest that the decrease in the Pauli repulsion (ΔE_{Pauli}) between r(C–F) = 6.0 Å and the transition structure is particularly large for the sterically most congested system $[F\cdots Me_3C\cdots F]^-$. This is quantitatively supported by the calculated change in the Pauli repulsion: $\Delta\Delta E_{Pauli} = -84.5$ kcal mol^{-1} (Table 2). Visual inspection also shows that the curves for ΔE_{int} and ΔE_{elstat} exhibit larger deviation when the central alkyl moiety is bulkier. To the extent that the Pauli term is related to steric repulsion, this is indeed a significant observation. It is interesting to note that the absolute values of ΔE_{Pauli} for all four TSs are very similar (Figure 3): that is, they are independent of the number of methyl groups attached to the central carbon atom. We do realize that the C–F bond lengths become longer when the size of the alkyl group increases. However a lengthening occurs both for the TS and for the reactant.

Table 2 shows that the changes in the interaction energy ($\Delta\Delta E_{int}$) between $r = 6.0$ and the transition structures in the systems $[F\cdots R_3C\cdots F]^-$ significantly decrease from $R_3 = H_3$ (−17.9 kcal mol^{-1}) to $R_3 = H_2Me$ (−13.6 kcal mol^{-1}), $R_3 = HMe_2$ (−6.2 kcal mol^{-1}) and $R_3 = Me_3$ (8.6 kcal mol^{-1}). The data also show that there is a concomitant *increase* in the alteration of the Pauli repulsion given by $\Delta\Delta E_{Pauli}$, from $R_3 = H_3$ (−55.5 kcal mol^{-1}) to $R_3 = H_2Me$ (−84.5 kcal mol^{-1}), $R_3 = HMe_2$ (−90.2 kcal mol^{-1}), and $R_3 = Me_3$ (−92.3 kcal mol^{-1}). As with the previous systems, the destabilizing forces in the transition structures come mainly from the weaker orbital interactions. The $\Delta\Delta E_{orb}$ values show the trend $R_3 = H_3$

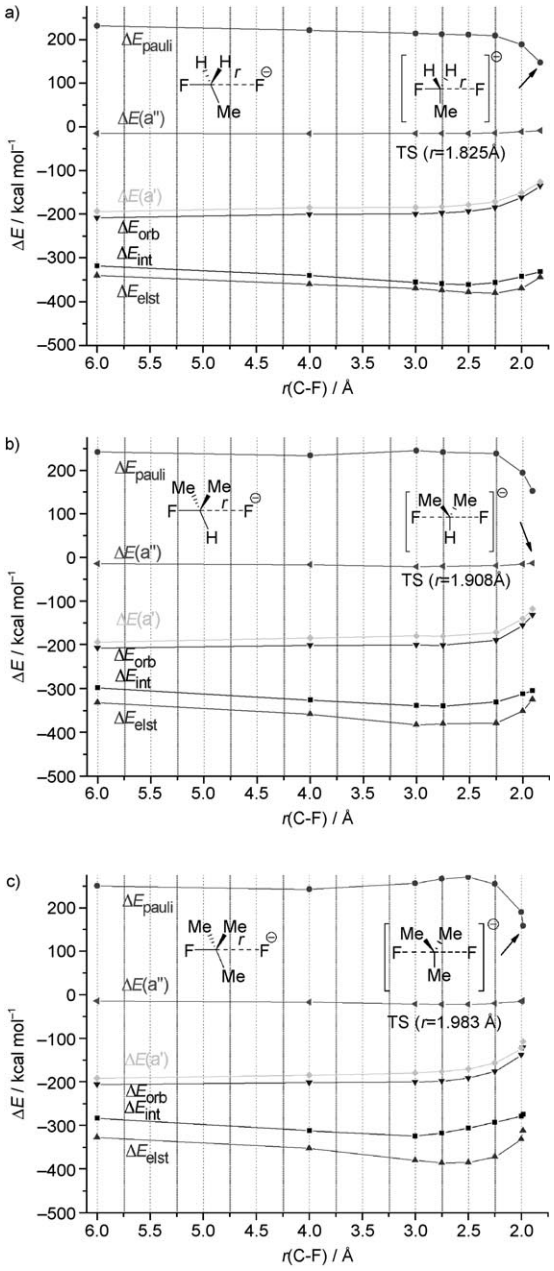

Figure 3. EDA plots for the RF+F$^-$ S_N2 reactions computed at the OPBE/TZ2P+ level. a) R = Et, b) R = *i*Pr, and c) R = *t*Bu.

(69.5 kcal mol^{-1}), $R_3 = H_2Me$ (74.3 kcal mol^{-1}), $R_3 = HMe_2$ (77.1 kcal mol^{-1}), and $R_3 = Me_3$ (85.6 kcal mol^{-1}). A significant contribution to the increase in the activation barrier also comes from the Coulomb interactions. The $\Delta\Delta E_{elstat}$ values (Table 2) show that the electrostatic attraction in the parent system with $R_3 = H_3$ increases in the transition structure by 31.9 kcal mol^{-1}. The contribution of $\Delta\Delta E_{elstat}$ is much smaller for $R_3 = H_2Me$ (−3.4 kcal mol^{-1}) and it becomes destabilizing in the transition structures of the bulkier systems. The calculated values are $R_3 = HMe_2$ (6.8 kcal mol^{-1}) and $R_3 = Me_3$ (15.4 kcal mol^{-1}). The latter values underline the crucial role of the Coulombic interaction for the trend of the activation energy in the system $[F\cdots R_3C\cdots F]^-$. We could not locate energy-minimum structures for the bulkier systems with $R_3 = H_2Me$, HMe_2 or Me_3, but the trend in the energy values for the different terms in the latter systems (Table 2) clearly indicates that the electrostatic attraction decreases and that the orbital term becomes significantly less stabilizing when approaching the transition structure.

Effect of the central atom: Although knowledge of pentacoordinated main group elements is old, Sølling and Radom were probably the first to apply quantum chemical methods to characterise identity S_N2 reactions without a central barrier ($E^{\#} = -E^0$; Figure 1).[43–45] The result is a single-well potential energy function in which the prototypical symmetric TS has become a potential energy minimum. This condition often occurs when the central atom is changed from carbon to main group elements of the third row, or for electropositive nucleophiles/electrofuges.[46,47] Bickelhaupt and coworkers elaborated on this idea and analysed the factors that control the shift from a reaction with a central barrier to a reaction without[33,48] Very recently they have devised a "ball-in-a-box" model to explain some of their findings.[33] From the perspective of the present investigation it would be particularly interesting to include some representative reactions at silicon, and thereby complement the work by Bickelhaupt.

We calculated the potential energy profiles of the following reactions at silicon, for comparison with the corresponding reactions at carbon [Reactions (1) and (2), above]:

$$F^- + SiH_3F \rightarrow FSiH_3 + F^- \quad (7)$$

$$Cl^- + SiH_3Cl \rightarrow ClSiH_3 + Cl^- \quad (8)$$

Our calculations led to single-well energy profiles, in accordance with the literature. This means that the (D_{3h}) pentacoordinated species $[X\cdots H_3E\cdots X]^-$ (X = F, Cl) in which both X–E distances have the same values are energy minima when E = Si, whereas when E = C they are transition structures. Furthermore, the results of OPBE and CCSD(T) are in good agreement for both reactions (Table 1).

Figure 4 shows that the curves for the total interaction energy (ΔE_{int}) and for the electrostatic attraction (ΔE_{elstat}) are very similar, both in the trend and—particularly for the chlorine system—also in the absolute values. The shapes of the curves make it obvious that in the latter system the attractive orbital interactions (ΔE_{orb}) and the Pauli term (ΔE_{Pauli}) at longer distances cancel and that the net attraction between r(Si–Cl) = 6.0 Å and 3.0 Å comes solely from the Coulomb term.[52] Note that between r(Si–Cl) = 3.0 Å and the equilibrium value the stabilization from ΔE_{elstat} is larger than the total interaction energy (Figure 4b), which means that the sum of the attractive and repulsive orbital interactions is overall slightly repulsive. A similar trend is displayed by the curves for the system $[F\cdots H_3Si\cdots F]^-$ (Figure 4a). It becomes clear that according to the EDA results

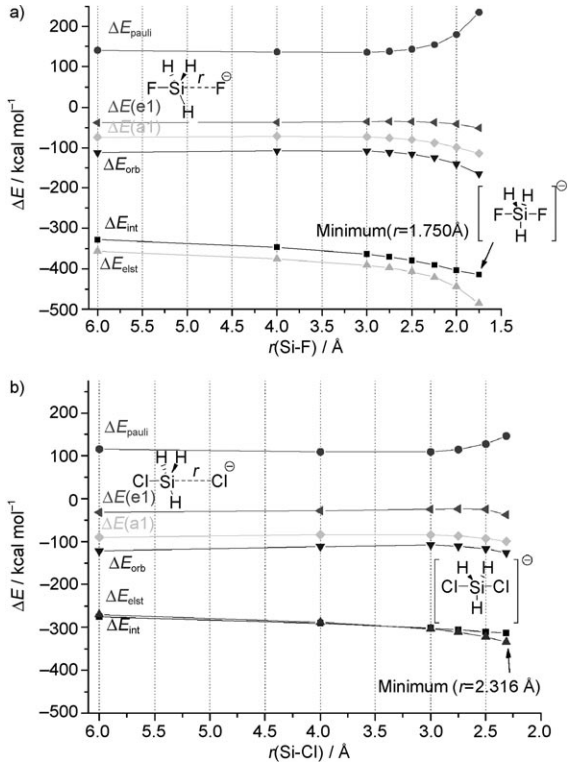

Figure 4. EDA plots for the SiH_3X+X^- S_N2 reactions computed at the OPBE/TZ2P+ level. a) X = F, b) R = Cl.

the Si–F and Si–Cl bonds have greater electrostatic than covalent character.

The numerical EDA results shown in Table 2 provide a more quantitative insight. The changes in the total attractive interaction energy between $r = 6.0$ Å and the equilibrium structures of the pentacoordinated complexes $[FSiH_3F]^-$ ($\Delta\Delta E_{int} = -86.5$ kcal mol^{-1}) and $[ClSiH_3Cl]^-$ ($\Delta\Delta E_{int} = -37.6$ kcal mol^{-1}) come mainly from the electrostatic attraction terms, which amount to $\Delta\Delta E_{elstat} = -128.0$ kcal mol^{-1} in $[FSiH_3F]^-$ and $\Delta\Delta E_{elstat} = -63.1$ kcal mol^{-1} in $[ClSiH_3Cl]^-$. The contributions of the attractive orbital interactions in $[FSiH_3F]^-$ ($\Delta\Delta E_{orb} = -52.9$ kcal mol^{-1}) and $[ClSiH_3Cl]^-$ ($\Delta\Delta E_{orb} = -5.0$ kcal mol^{-1}) are considerably less. It is interesting to note that the change in the Pauli repulsion ($\Delta\Delta E_{Pauli}$) along the reaction coordinate $[XH_3Si\cdots X]^-$ destabilizes the formation of the pentacoordinated energy minima $[XSiH_3X]^-$ whereas in the carbon systems $[XH_3CX]^-$ it stabilizes the formation of the transition structure.

Discussion

The EDA results we present here shed light on the S_N2 reaction and offer a new interpretation of the factors governing the reaction course and the barrier height. They also provide a detailed account of the factors that make the D_{3h} structures of the carbon systems $[X–H_3C–X]^-$ transition structures whereas the silicon homologues $[X–H_3Si–X]^-$ are energy minima. We want to point out that this work does not invalidate previous work. Our study offers a new perspective that comes from the choice of the reference system in which the newly formed bond and the breaking bond in the S_N2 reaction are analysed simultaneously. We think that this is perhaps a more reasonable choice for a reference system than focussing mainly on the bond-formation between the attacking nucleophile and the reagent. In particular, the role of the steric repulsion over the course of the reaction is seen in a different light.

The EDA results for the S_N2 Reactions (1)–(5) for carbon systems show that there are decreases in ΔE_{Pauli} upon going from reactants to TSs, indicating less steric hindrance in the TSs than in the substrates. In other words, the umbrella inversion mechanism is not unfavourable in terms of steric hindrance at the TS as often assumed in, for example, text books. This result comes to the fore when not only the interaction between the nucleophile X^- and the substrate CR_3X is considered, but also the change in the interaction between the leaving X^- and the remaining fragment. The results for Reactions (1)–(5) are unique in showing that if it were for the Pauli component only, bulkier substrates would always give rise to faster reactions! In other words, the usually observed normal reactivity trend—$CH_3 > CH_3CH_2 > (CH_3)_2CH > (CH_3)_3C$—is the result of the electrostatic and orbital terms rather than the Pauli component in our energy decomposition scheme. In this respect, the use of the term "steric hindrance" to describe the phenomenon is highly unfortunate. According to the IUPAC, the steric effect in a reaction is attributable to the difference in steric energy between, on the one hand, reactants and, on the other hand, the transition structure. In the present context this definition is of little use.

We realize that it is difficult, both in principle and in practice, to apply experimental methods to disentangle a steric effect term due to increasing number and size of substituent alkyl groups from the corresponding electronic effect. One part of the enigma is the evident fact that the presence of an extra alkyl group increases both the sheer size of the molecule and the electronic structure at the reactive centre. In that respect, systematic and reliable quantum chemical calculations of the reactivities of carefully chosen model systems appear more attractive. A recently published paper on the gas-phase reactivities of remotely substituted allylic substrates represents an example of this approach.[49] The analysis revealed that the electronic effect associated with substitution of methyl groups for hydrogen atoms at the central carbon is at least of the same magnitude as the steric effect. Secondly, there are cases in which the order in reaction rate is opposite from the normal. This perplexing situation is well documented for the cationic S_N2 reactions $H_2O+ROH_2^+$ and $HF+RFH^+$,[50,51] and the fact that the *tert*-butyl substrate in the former case reacts more rapidly than the smaller alkyl substrates can obviously not be explained which reference to any steric effect. We realize that there will be one steric effect on the substrate and a differ-

ent one on the TS, and the critical energy represents exactly this difference.

The comparison of the EDA results for the carbon systems $[XH_3C\cdots X]^-$ with those for the silicon homologues $[XH_3Si\cdots X]^-$ for X=F, Cl reveals striking differences between the two series, which are enlightening because of the choice of the reference system. The formation of the D_{3h} structures as transition structures for the carbon compounds is actually facilitated by reduced steric repulsion and by stronger electrostatic attraction, as indicated by the negative values for $\Delta\Delta E_{Pauli}$ and for $\Delta\Delta E_{elstat}$ between $r=6.0$ Å and the transition structure (Table 2). The contribution of the electrostatic attraction in the transition structure is weaker than in the energy-minimum structure, but the largest contribution to the energy increase in the transition structure comes from the orbital term ($\Delta\Delta E_{orb}$). The crucial factor that leads to overall energy increases in the carbon systems is thus the destabilizing contribution from these orbital interactions.

Another important finding concerns the changes in the geometries of the interacting fragments. Table 2 shows that the $\Delta\Delta E_{prep}$ values for the D_{3h} transition structures of the carbon systems are less positive than for the energy minima. For the silicon homologues $[XH_3Si\cdots X]^-$, the formation of the D_{3h} energy minima is driven by the large increases in the electrostatic interactions between $r=6.0$ Å and the equilibrium structures ($\Delta\Delta E_{elstat}$) and also by stronger orbital interactions ($\Delta\Delta E_{orb}$), while the change in the steric interactions ($\Delta\Delta E_{Pauli}$) is destabilizing.

The results also show that a chemical bond—irrespective of whether it is strong and covalent or weak and dispersive—is always the result of a compromise between an attractive and a repulsive force. Although the Hamiltonian of a molecular system is simple in principle, the origin of the attractive and repulsive contributions is a highly complex matter. This study illustrates how the EDA provides a systematic method to describe these terms using a set of physically well defined terms.

Conclusions

The EDA results for the prototypical S_N2 reactions of the systems $[X\cdots R_3E\cdots X]^-$ in which the interacting fragments are $[X\cdots X]^{2-}$ and $[R_3E]^+$ have given rise to a new interpretation of the factors governing the courses of the reactions. The EDA results for the carbon systems (E=C) show that there is less steric repulsion and stronger electrostatic attraction in the transition structures than in the precursor complexes and that the energy increases come mainly from weaker orbital interactions. The larger barriers for the systems when R_3 becomes bulkier also do not arise from more steric repulsion, which in the transition structure is actually released. It is rather the weakening of the electrostatic attraction, and in particular the loss of attractive orbital interactions, that are responsible for the activation barrier. The D_{3h} energy minima of the silicon homologues $[XH_3SiX]^-$ are driven by the large increases in the electrostatic interactions and also by stronger orbital interactions, whereas the steric interactions are destabilizing.

Acknowledgement

The authors are grateful to Professor Inge Røeggen for valuable comments. This work was supported by the Deutsche Forschungsgemeinschaft. I.F. is a Ramón y Cajal fellow.

[1] C. K. Ingold, *Structure and Mechanism in Organic Chemistry*, Cornell University, Ithaca, **1953**.
[2] T. H. Lowry, K. S. Richardson, *Mechanism and Theory in Organic Chemistry*, 2nd ed., Harper & Row, New York, **1981**.
[3] J. March, *Advanced Organic Chemistry*, 4th ed., Wiley, New York, **1992**.
[4] N. Isaacs, *Physical Organic Chemistry*, 2nd ed., Longman Scientific, Burnt Mill, **1995**.
[5] G. Frenking, A. Krapp, *J. Comput. Chem.* **2007**, *28*, 15.
[6] J. K. Laerdahl, E. Uggerud, *Int. J. Mass Spectrom.* **2002**, *214*, 277.
[7] L. B. Young, E. Lee-Ruff, D. K. Bohme, *J. Chem. Soc. Chem. Commun.* **1973**, 35.
[8] J. L. Beauchamp, M. C. Caserio, T. B. McMahon, *J. Am. Chem. Soc.* **1974**, *96*, 6243.
[9] D. K. Bohme, G. I. Mackay, J. D. Payzant, *J. Am. Chem. Soc.* **1974**, *96*, 4027.
[10] J. I. Brauman, W. N. Olmstead, C. A. Lieder, *J. Am. Chem. Soc.* **1974**, *96*, 4030.
[11] K. Hiraoka, P. Kebarle, *J. Am. Chem. Soc.* **1976**, *98*, 6119.
[12] D. K. Bohme, G. I. Mackay, *J. Am. Chem. Soc.* **1981**, *103*, 978.
[13] M. L. Chabinyc, S. L. Craig, C. K. Regan, J. I. Brauman, *Science* **1998**, *279*, 1882.
[14] S. Wolfe, D. J. Mitchell, H. B. Schlegel, *J. Am. Chem. Soc.* **1981**, *103*, 7692.
[15] S. Wolfe, D. J. Mitchell, H. B. Schlegel, *J. Am. Chem. Soc.* **1981**, *103*, 7694.
[16] K. Morokuma, *J. Am. Chem. Soc.* **1982**, *104*, 3732.
[17] A. Pross, S. Shaik, *Acc. Chem. Res.* **1983**, *16*, 363.
[18] S. Shaik, H. B. Schlegel, S. Wolfe, *Theoretical Aspects of Physical Organic Chemistry: The S_N2 Reaction*, Wiley, New York, **1992**.
[19] S. Hoz, H. Basch, J. L. Wolk, T. Hoz, E. Rozental, *J. Am. Chem. Soc.* **1999**, *121*, 7724.
[20] R. Yi, H. Basch, S. Hoz, *J. Org. Chem.* **2002**, *67*, 5891.
[21] E. Uggerud, *Chem. Eur. J.* **2006**, *12*, 1127.
[22] L. G. Arnaut, A. A. C. C. Pais, S. J. Formosinho, *J. Mol. Struct.* **2001**, *563–564*, 1.
[23] K. Morokuma, *J. Chem. Phys.* **1971**, *55*, 1236.
[24] T. Ziegler, A. Rauk, *Theor. Chem. Acc.* **1977**, *46*, 1.
[25] Conjugation and hyperconjugation: a) D. Cappel, S. Tüllmann, A. Krapp, G. Frenking, *Angew. Chem.* **2005**, *117*, 3683; *Angew. Chem. Int. Ed.* **2005**, *44*, 3617; b) I. Fernández, G. Frenking, *Chem. Eur. J.* **2006**, *12*, 3617; c) I. Fernández, G. Frenking, *J. Org. Chem.* **2006**, *71*, 2251; d) I. Fernández, G. Frenking, *Chem. Commun.* **2006**, 5030; e) I. Fernández, G. Frenking, *J. Phys. Chem. A* **2007**, *111*, 8028; f) I. Fernández, G. Frenking, *J. Org. Chem.* **2007**, *72*, 7367.
[26] Aromaticity: a) I. Fernández, G. Frenking, *Faraday Discuss.* **2007**, *135*, 403; b) I. Fernández, G. Frenking, *Chem. Eur. J.* **2007**, *13*, 5873.
[27] G. Frenking, K. Wichmann, N. Frohlich, C. Loschen, M. Lein, J. Frunzke, V. M. Rayón, *Coord. Chem. Rev.* **2003**, *238–239*, 55.
[28] M. Lein, G. Frenking in *Theory and Applications of Computational Chemistry: The First 40 Years* (Eds.: C. E. Dykstra, G. Frenking, K. S. Kim, G. E. Scuseria), Elsevier, Amsterdam, **2005**, pp. 291.
[29] Theoretical Chemistry Accounts: Theory, Computation, and Modeling C. Esterhuysen, G. Frenking, *Theor. Chim. Acta* **2004**, *111*, 381.
[30] A. Kovács, C. Esterhuysen, G. Frenking, *Chem. Eur. J.* **2005**, *11*, 1813.

[31] A. Krapp, F. M. Bickelhaupt, G. Frenking, *Chem. Eur. J.* **2006**, *12*, 9196.
[32] F. M. Bickelhaupt, *J. Comput. Chem.* **1999**, *20*, 114.
[33] S. C. A. H. Pierrefixe, C. F. Guerra, F. M. Bickelhaupt, *Chem. Eur. J.* **2008**, *14*, 819.
[34] a) N. C. Handy, J. A. Cohen, *Mol. Phys.* **2001**, *99*, 403; b) J. P. Perdew, K. Burke, M. Ernzerhof, *Phys. Rev. Lett.* **1996**, *77*, 3865.
[35] M. Swart, M. Solá, F. M. Bickelhaupt, *J. Comput. Chem.* **2007**, *28*, 1551.
[36] J. G. Snijders, E. J. Baerends, P. Vernooijs, *At. Data Nucl. Data Tables* **1981**, *26*, 483.
[37] J. Krijn, E. J. Baerends, *Fit Functions in the HFS-Method*, Vrije Universiteit, Amsterdam, **1984**.
[38] E. J. Baerends, Scientific Computing & Modelling NV, Amsterdam, **2007**.
[39] F. Weigend, R. Alhrichs, *Phys. Chem. Chem. Phys.* **2005**, *7*, 3297.
[40] Gaussian 03, Revision D.01, M. J. Frisch, G. W. Trucks, H. B. Schlegel, G. E. Scuseria, M. A. Robb, J. R. Cheeseman, J. A. Montgomery, Jr., T. Vreven, K. N. Kudin, J. C. Burant, J. M. Millam, S. S. Iyengar, J. Tomasi, V. Barone, B. Mennucci, M. Cossi, G. Scalmani, N. Rega, G. A. Petersson, H. Nakatsuji, M. Hada, M. Ehara, K. Toyota, R. Fukuda, J. Hasegawa, M. Ishida, T. Nakajima, Y. Honda, O. Kitao, H. Nakai, M. Klene, X. Li, J. E. Knox, H. P. Hratchian, J. B. Cross, V. Bakken, C. Adamo, J. Jaramillo, R. Gomperts, R. E. Stratmann, O. Yazyev, A. J. Austin, R. Cammi, C. Pomelli, J. W. Ochterski, P. Y. Ayala, K. Morokuma, G. A. Voth, P. Salvador, J. J. Dannenberg, V. G. Zakrzewski, S. Dapprich, A. D. Daniels, M. C. Strain, O. Farkas, D. K. Malick, A. D. Rabuck, K. Raghavachari, J. B. Foresman, J. V. Ortiz, Q. Cui, A. G. Baboul, S. Clifford, J. Cioslowski, B. B. Stefanov, G. Liu, A. Liashenko, P. Piskorz, I. Komaromi, R. L. Martin, D. J. Fox, T. Keith, M. A. Al-Laham, C. Y. Peng, A. Nanayakkara, M. Challacombe, P. M. W. Gill, B. Johnson, W. Chen, M. W. Wong, C. Gonzalez, J. A. Pople, Gaussian, Inc., Wallingford CT, **2004**.
[41] W. N. Olmstead, J. I. Brauman, *J. Am. Chem. Soc.* **1977**, *99*, 4219.
[42] M. Swart, A. W. Ehlers, K. Lammertsma, *Mol. Phys.* **2004**, *102*, 2467.
[43] a) T. I. Sølling, A. Pross, L. Radom, *Int. J. Mass Spectrom.* **2001**, *210*, 1; b) T. I. Solling, S. B. Wild, L. Radom, *Inorg. Chem.* **1999**, *38*, 6049.
[44] T. I. Sølling, L. Radom, *Chem. Eur. J.* **2001**, *7*, 1516.
[45] T. I. Sølling, L. Radom, *Eur. J. Mass Spectrom.* **2000**, *6*, 153.
[46] J. Z. Dávalos, R. Herrero, J.-L. M. Abboud, O. Mó, M. Yáñez, *Angew. Chem.* **2007**, *119*, 385; *Angew. Chem. Int. Ed.* **2007**, *46*, 381.
[47] I. Fernández, E. Uggerud, G. Frenking, *Chem. Eur. J.* **2007**, *13*, 8620.
[48] M. A. van Bochove, M. Swart, F. M. Bickelhaupt, *J. Am. Chem. Soc.* **2006**, *128*, 10738.
[49] R. A. Ochran, E. Uggerud, *Int. J. Mass Spectrom.* **2007**, *265*, 169.
[50] J. K. Laerdahl, E. Uggerud, *Org. Biomol. Chem.* **2003**, *1*, 2935.
[51] J. K. Laerdahl, P. U. Civcir, L. Bache-Andreassen, E. Uggerud, *Org. Biomol. Chem.* **2006**, *4*, 135.
[52] It is of course arbitrary to sum up the Pauli repulsion ΔE_{Pauli} to the orbital term ΔE_{orb} an to declare the electrostatic attraction ΔE_{elst} as the sole origin for the net attraction. It can be justified by arguing that ΔE_{Pauli} gives the repulsive interactions between occupied orbitals while ΔE_{orb} gives the attractive interactions between vacant and occupied orbitals.

Received: September 4, 2008
Published online: January 13, 2009

